INTERNATIONAL JOURNAL FOR NUMERICAL METHODS IN FLUIDS, VOL. 8, 743–758 (1988)

MAGNETOHYDRODYNAMIC FLOW ON A HALF-PLANE

MÜNEVVER SEZGIN
Department of Mathematics, Middle East Technical University, Ankara, Turkey

SUMMARY

We investigate the magnetohydrodynamic flow (MHD) on the upper half of a non-conducting plane for the case when the flow is driven by the current produced by an electrode placed in the middle of the plane. The applied magnetic field is perpendicular to the plane, the flow is laminar, uniform, steady and incompressible. An analytical solution has been developed for the velocity field and the induced magnetic field by reducing the problem to the solution of a Fredholm's integral equation of the second kind, which has been solved numerically. Infinite integrals occurring in the kernel of the integral equation and in the velocity and magnetic field were approximated for large Hartmann numbers by using Bessel functions. As the Hartmann number M increases, boundary layers are formed near the non-conducting boundaries and a parabolic boundary layer is developed in the interface region. Some graphs are given to show examples of this behaviour.

KEY WORDS MHD Flow Half-plane

FORMULATION OF THE PROBLEM

We consider the steady flow of an incompressible fluid with uniform prroperties driven by the interaction of imposed electric currents and a uniform transverse magnetic field. Imposed currents enter the fluid at $\xi = \pm a_1$ through external circuits and move up on the plane. We assume that all the physical variables, including pressure, and the boundary conditions are functions of ξ and η only. The pressure gradient is zero. There is only one component of velocity and of magnetic field (in the z-direction). The equations describing such flows are the same as those of MHD duct flow problems when pressure gradient is taken as zero. Figure 1 shows the geometry of the problem.

A uniform magnetic field of strength H_0 is directed along the axis of η. The wall is electrically insulated except for a length $2a_1$ in the middle, where a perfectly conducting electrode is placed so that this part is conducting. Thus the partial differential equations describing the flow (in non-dimensionalized form) are[1, 2]

$$\nabla^2 V + M(\partial B/\partial \eta) = 0, \tag{1}$$

$$\nabla^2 B + M(\partial V/\partial \eta) = 0, \tag{2}$$

with the boundary conditions

$$V = 0; \quad \eta = 0, \tag{3a}$$

$$|V| < \infty, \qquad |B| < \infty \quad \text{as} \quad \eta \to \infty, \tag{3b}$$

$$B = 1; \quad \eta = 0, a_1 < \xi < \infty, \tag{3c}$$

0271–2091/88/070743–16$08.00

Received 2 December 1986
Revised 13 August 1987

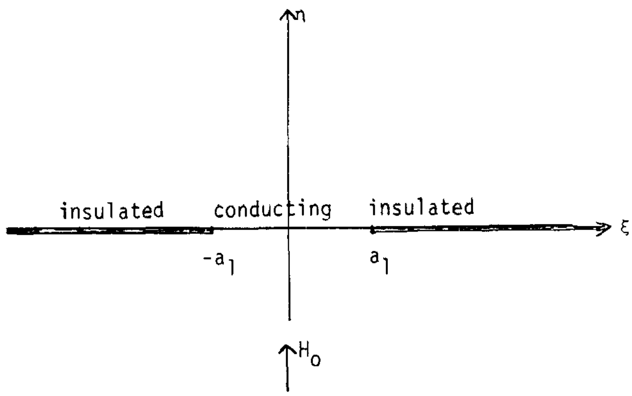

Figure 1. The geometry of the problem

$$B=-1;\quad \eta=0,\ -\infty<\xi<-a_1, \tag{3d}$$

$$\partial B/\partial\eta=0;\quad \eta=0,\ -a_1<\xi<a_1. \tag{3e}$$

In Hunt and Williams' paper[3] the MHD flow between two parallel non-conducting planes was investigated for the case when the flow is driven by the current produced by electrodes placed one in each plane, the applied magnetic field being perpendicular to the planes. In this study we have considered a more general problem by taking one of the planes as partially insulated, partially perfectly conducting and assuming the other plane to be at infinity.

METHOD OF SOLUTION

We take Fourier sine transforms of $V(\xi,\eta)$ and $B(\xi,\eta)$ as

$$\bar{V}(\alpha,\eta)=\int_0^\infty V(\xi,\eta)\sin(\xi\alpha)\mathrm{d}\xi, \tag{4}$$

$$\bar{B}(\alpha,\eta)=\int_0^\infty B(\xi,\eta)\sin(\xi\alpha)\mathrm{d}\xi. \tag{5}$$

Then

$$V(\xi,\eta)=\frac{2}{\pi}\int_0^\infty \bar{V}(\alpha,\eta)\sin(\xi\alpha)\mathrm{d}\alpha, \tag{6}$$

$$B(\xi,\eta)=\frac{2}{\pi}\int_0^\infty \bar{B}(\alpha,\eta)\sin(\xi\alpha)\mathrm{d}\alpha. \tag{7}$$

By taking the Fourier sine transforms of the equations (1) and (2), we get the partial differential equations for $\bar{V}$ and $\bar{B}$ as

$$\partial^2\bar{V}/\partial\eta^2-\alpha^2\bar{V}+M(\partial\bar{B}/\partial\eta)=0, \tag{8}$$

$$\partial^2\bar{B}/\partial\eta^2-\alpha^2\bar{B}+M(\partial\bar{V}/\partial\eta)=0, \tag{9}$$

and the boundary conditions (3) imply

$$\bar{V}(\alpha,0)=0, \tag{10}$$

$$|\bar{V}| < \infty, \qquad |\bar{B}| < \infty \quad \text{as } \eta \to \infty. \tag{11}$$

The general solution of the equations (8) and (9) is given as

$$\begin{aligned}\bar{V}(\alpha,\eta) &= \mathrm{e}^{-M\eta/2}[A(\alpha)(\mathrm{e}^{\mu_\alpha\eta}+\mathrm{e}^{-\mu_\alpha\eta})+B(\alpha)(\mathrm{e}^{\mu_\alpha\eta}-\mathrm{e}^{-\mu_\alpha\eta})]/2\\ &\quad +\mathrm{e}^{+M\eta/2}[C(\alpha)(\mathrm{e}^{\mu_\alpha\eta}+\mathrm{e}^{-\mu_\alpha\eta})+D(\alpha)(\mathrm{e}^{\mu_\alpha\eta}-\mathrm{e}^{-\mu_\alpha\eta})]/2,\end{aligned} \tag{12}$$

$$\begin{aligned}\bar{B}(\alpha,\eta) &= \mathrm{e}^{-M\eta/2}[A(\alpha)(\mathrm{e}^{\mu_\alpha\eta}+\mathrm{e}^{-\mu_\alpha\eta})+B(\alpha)(\mathrm{e}^{\mu_\alpha\eta}-\mathrm{e}^{-\mu_\alpha\eta})]/2\\ &\quad -\mathrm{e}^{M\eta/2}[C(\alpha)(\mathrm{e}^{\mu_\alpha\eta}+\mathrm{e}^{-\mu_\alpha\eta})+D(\alpha)(\mathrm{e}^{\mu_\alpha\eta}-\mathrm{e}^{-\mu_\alpha\eta})]/2,\end{aligned} \tag{13}$$

where

$$\mu_\alpha = (M^2/4+\alpha^2)^{1/2}. \tag{14}$$

Applying the boundary conditions, the number of unknowns is reduced to one and we get

$$\bar{V}(\alpha,\eta) = -2A(\alpha)\mathrm{e}^{-\mu_\alpha\eta}\mathrm{sh}(M\eta/2), \tag{15}$$

$$\bar{B}(\alpha,\eta) = 2A(\alpha)\mathrm{e}^{-\mu_\alpha\eta}\mathrm{ch}(M\eta/2), \tag{16}$$

where $\mathrm{sh}(x)$ and $\mathrm{ch}(x)$ are sine and cosine hyperbolic functions respectively.

Then from equations (6) and (7) V and B are obtained as

$$V(\xi,\eta) = -\frac{4}{\pi}\int_0^\infty A(\alpha)\mathrm{e}^{-\mu_\alpha\eta}\mathrm{sh}(M\eta/2)\sin(\xi\alpha)\,\mathrm{d}\alpha, \tag{17}$$

$$B(\xi,\eta) = \frac{4}{\pi}\int_0^\infty A(\alpha)\mathrm{e}^{-\mu_\alpha\eta}\mathrm{ch}\left(\frac{M\eta}{2}\right)\sin(\xi\alpha)\,\mathrm{d}\alpha. \tag{18}$$

From the mixed boundary conditions (3c, d, e) one can obtain the following dual integral equations:

$$\int_0^\infty A(\alpha)\sin(\xi\alpha)\,\mathrm{d}\alpha = \frac{\pi}{4}; \quad a_1 < \xi < \infty, \tag{19}$$

$$\int_0^\infty \mu_\alpha A(\alpha)\sin(\xi\alpha)\,\mathrm{d}\alpha = 0; \quad 0 < \xi < a_1. \tag{20}$$

In view of the antisymmetry about the line $\xi = 0$, we need to consider the solution in the region $0 \leqslant \xi < \infty$ only.

SOLUTION OF DUAL INTEGRAL EQUATIONS

Let the representation for $A(\alpha)$ be

$$A(\alpha) = J_0(\alpha a_1)/2\alpha + H(\alpha). \tag{21}$$

Then dual integral equations (19) and (20) are obtained in terms of $H(\alpha)$ as

$$\int_0^\infty H(\alpha)\sin(\xi\alpha)\,\mathrm{d}\alpha = 0; \quad a_1 < \xi < \infty, \tag{22}$$

$$\int_0^\infty \mu_\alpha H(\alpha)\sin(\xi\alpha)\,\mathrm{d}\alpha = -\int_0^\infty \frac{\mu_\alpha}{2\alpha} J_0(\alpha a_1)\sin(\xi\alpha)\,\mathrm{d}\alpha; \quad 0 < \xi < a_1, \tag{23}$$

where $J_0(x)$, $J_1(x)$ are Bessel functions of the first kind of order zero and one respectively.

We choose a representation for the unknown $H(\alpha)$ now as

$$H(\alpha)=\int_0^{a_1} xf(x)J_1(\alpha x)\mathrm{d}x. \tag{24}$$

Since the dual integral equations (22) and (23) can be written as (after equation (23) has been integrated with respect to ξ from 0 to ξ)

$$\int_0^{\infty} H(\alpha)\sin(\xi\alpha)\mathrm{d}\alpha=0; \quad a_1<\xi<\infty, \tag{25}$$

$$\int_0^{\infty} \mu_\alpha H_\alpha \frac{1-\cos(\xi\alpha)}{\alpha}\mathrm{d}\alpha=-\frac{1}{2}\int_0^{\infty}\frac{\mu_\alpha}{\alpha}J_0(\alpha a_1)\frac{1-\cos(\xi\alpha)}{\alpha}\mathrm{d}\alpha; \quad 0<\xi<a_1, \tag{26}$$

the first integral equation (25) is automatically satisfied by this representation (equation (24)) of $H(\alpha)$ by virtue of the identity

$$\int_0^{\infty} J_1(st)\sin(sx)\,\mathrm{d}s=\frac{x}{t}\frac{H(t-x)}{(t^2-x^2)^{1/2}}, \tag{27}$$

and, with the help of the identity[4]

$$\int_0^{\infty} J_1(st)\cos(sx)\mathrm{d}s=\frac{1}{t}-\frac{x}{t}\frac{H(x-t)}{(x^2-t^2)^{1/2}}, \tag{28}$$

the second integral equation (26) is reduced to an Abel's integral equation by substituting $H(\alpha)$ from equation (24):

$$\int_0^{\infty}\frac{f(x)}{(\xi^2-x^2)^{1/2}}\mathrm{d}x=h(\xi); \quad 0<\xi<a_1, \tag{29}$$

where

$$h(\xi)=\frac{1}{\xi}\int_0^{a_1} f(x)\mathrm{d}x+\frac{1}{\xi}\int_0^{\infty}\frac{\mu_\alpha}{2\alpha^2}J_0(\alpha a_1)[1-\cos(\xi\alpha)]\mathrm{d}\alpha$$
$$+\frac{1}{\xi}\int_0^{a_1} xf(x)\int_0^{\infty}\frac{\mu_\alpha}{\alpha}J_1(\alpha x)[1-\cos(\xi\alpha)]\mathrm{d}\alpha\mathrm{d}x. \tag{30}$$

The solution of Abel's integral equation (29) is given by[5]

$$f(x)=\frac{2}{\pi}\frac{\mathrm{d}}{\mathrm{d}x}\int_0^{x}\frac{\xi h(\xi)}{(x^2-\xi^2)^{1/2}}\mathrm{d}\xi. \tag{31}$$

Substitution of $h(\xi)$ from (30) with the help of some known identities[6] reduces equation (31) to a Fredholm's integral equation of the second kind for $f(t)$:

$$\rho\theta(\rho)+\int_0^{1} K(\rho,t)t\theta(t)\mathrm{d}t=\rho p(\rho), \tag{32}$$

where the kernel $K(\rho,t)$ and the free term $p(\rho)$ are

$$K(\rho,t)=a_1^2\rho\int_0^{\infty}\left[\left(\frac{M^2}{4}+\alpha^2\right)^{1/2}-\alpha\right]J_1(\alpha t a_1)J_1(\alpha\rho a_1)\mathrm{d}\alpha, \tag{33}$$

$$p(\rho)=-\frac{1}{2}\int_0^{\infty}\frac{1}{\alpha}\left(\frac{M^2}{4}+\alpha^2\right)^{1/2}J_1(\alpha\rho a_1)\mathrm{d}\alpha \tag{34}$$

and

$$\rho\theta(\rho)=\rho f(\rho a_1)-1/2a_1;\quad 0<\rho<1. \tag{35}$$

At this point we notice that the infinite integrals in the kernel and the right-hand-side function are slowly convergent and oscillating due to the Bessel functions J_0, J_1. Both of these integrals are almost impossible to compute numerically; therefore we look for methods to convert them into more easily computable form.

With the help of the identities[7,8]

$$J_1(\alpha\rho a_1)J_1(\alpha t a_1)=\frac{1}{\pi}\int_0^{\pi} e^{-i\theta}J_0(\alpha a_1 r)d\theta, \tag{36}$$

$$\int_0^{\infty}\left[\left(\frac{M^2}{4}+\alpha^2\right)^{1/2}-\alpha\right]J_0(\alpha a_1 r)d\alpha=\frac{M^2}{8}\left[I_0\left(\frac{Ma_1}{4}r\right)K_0\left(\frac{Ma_1}{4}r\right)+I_1\left(\frac{Ma_1}{4}r\right)K_1\left(\frac{Ma_1}{4}r\right)\right] \tag{37}$$

and the identity (obtained in Appendix I)

$$\begin{aligned}\int_0^{\infty}\frac{1}{\alpha}\left(\frac{M^2}{4}+\alpha^2\right)^{1/2}J_1(\alpha a_1\rho)d\alpha\\ =\frac{M}{4}\left\{\frac{M}{2}a_1\rho\left[I_0\left(\frac{Ma_1}{4}\rho\right)K_0\left(\frac{Ma_1}{4}\rho\right)+I_1\left(\frac{Ma_1}{4}\rho\right)K_1\left(\frac{Ma_1}{4}\rho\right)\right]\right.\\ \left.+I_0\left(\frac{Ma_1}{4}\rho\right)K_1\left(\frac{Ma_1}{4}\rho\right)-I_1\left(\frac{Ma_1}{4}\rho\right)K_0\left(\frac{Ma_1}{4}\rho\right)\right\},\end{aligned} \tag{38}$$

where

$$r^2=\rho^2+t^2-2\rho t\cos\theta \tag{39}$$

and $I_0(x)$, $I_1(x)$, $K_0(x)$, $K_1(x)$ are Modified Bessel functions of the first and second kind of order zero and one respectively, the Fredholm's integral equation (32) can be written as

$$\rho\theta(\rho)+\int_0^1 K(\rho,t)t\theta(t)=\rho p(\rho), \tag{40}$$

where

$$K(\rho,t)=a_1^2\rho\frac{M^2}{8\pi}\int_0^{\pi}\cos\theta\left[I_0\left(\frac{Ma_1}{4}r\right)K_0\left(\frac{Ma_1}{4}r\right)+I_1\left(\frac{Ma_1}{4}r\right)K_1\left(\frac{Ma_1}{4}r\right)\right]d\theta \tag{41}$$

$$\begin{aligned}p(\rho)=-\frac{M}{8}\left\{\frac{M}{2}a_1\rho\left[I_0\left(\frac{Ma_1}{4}\rho\right)K_0\left(\frac{Ma_1}{4}\rho\right)+I_1\left(\frac{Ma_1}{4}\rho\right)K_1\left(\frac{Ma_1}{4}\rho\right)\right]\right.\\ \left.+I_0\left(\frac{Ma_1}{4}\rho\right)K_1\left(\frac{Ma_1}{4}\rho\right)-I_1\left(\frac{Ma_1}{4}\rho\right)K_0\left(\frac{Ma_1}{4}\rho\right)\right\}.\end{aligned} \tag{42}$$

The kernel and the right-hand side are now much more easily computable than before.

To solve the Fredholm's integral equation (40), we replace the integral by a Gaussian-based numerical quadrature and a system of algebraic equations is obtained for the unknown function θ and therefore f through equation (35).

By virtue of the equations for $H(\alpha)$ (equation (24)) and $A(\alpha)$ (equation (21)), the velocity $V(\xi,\eta)$ and the magnetic field $B(\xi,\eta)$ can be found through equations (17) and (18) in terms of $\rho\theta(\rho)$. So after changing the order of integrations, we get

$$V(\xi,\eta)=-\frac{4}{\pi}\,\mathrm{sh}\left(\frac{M\eta}{2}\right)a_1^2\int_0^1\rho\theta(\rho)\int_0^\infty J_1(\alpha\rho a_1)\mathrm{e}^{-\mu_\alpha\eta}\sin(\xi\alpha)\mathrm{d}\alpha\,\mathrm{d}\rho$$
$$-\frac{2}{\pi}\,\mathrm{sh}\left(\frac{M\eta}{2}\right)\int_0^\infty \mathrm{e}^{-\mu_\alpha\eta}\frac{\sin(\xi\alpha)}{\alpha}\mathrm{d}\alpha, \tag{43}$$

$$B(\xi,\eta)=\frac{4}{\pi}\,\mathrm{ch}\left(\frac{M\eta}{2}\right)a_1^2\int_0^1\rho\theta(\rho)\int_0^\infty J_1(\alpha\rho a_1)\mathrm{e}^{-\mu_\alpha\eta}\sin(\xi\alpha)\mathrm{d}\alpha\,\mathrm{d}\rho$$
$$+\frac{2}{\pi}\,\mathrm{ch}\left(\frac{M\eta}{2}\right)\int_0^\infty \mathrm{e}^{-\mu_\alpha\eta}\frac{\sin(\xi\alpha)}{\alpha}\mathrm{d}\alpha. \tag{44}$$

Now the infinite integrals in V and B can also be transformed to finite integrals which are much more easily computable. For these integrals we use the identities (obtained in Appendix II)

$$\int_0^\infty \mathrm{e}^{-k\left(\frac{M^2}{4}+\alpha^2\right)^{1/2}}\sin(\xi\alpha)J_1(\alpha x)\mathrm{d}\alpha=-\frac{Mk}{2\pi}\int_0^\infty\cos\theta\frac{K_1\{(M/2)[(\xi+x\cos\theta)^2+k^2]^{1/2}\}}{[(\xi+x\cos\theta)^2+k^2]^{1/2}}\mathrm{d}\theta \tag{45}$$

and[9]

$$\int_0^\infty \mathrm{e}^{-k(M^2/4+\alpha^2)^{1/2}}\frac{\sin(\xi\alpha)}{\alpha}\mathrm{d}\alpha=\int_0^\xi\frac{Mk}{2(t^2+k^2)^{1/2}}K_1\left(\frac{M}{2}(t^2+k^2)^{1/2}\right)\mathrm{d}t. \tag{46}$$

Thus $V(\xi,\eta)$, $B(\xi,\eta)$ can be written as

$$V(\xi,\eta)=\frac{2M\eta}{\pi^2}\,\mathrm{sh}\left(\frac{M\eta}{2}\right)a_1^2\int_0^1\rho\theta(\rho)\int_0^\pi\cos\theta\frac{K_1\{(M/2)[(\xi+a_1\rho\cos\theta)^2+\eta^2]^{1/2}\}}{[(\xi+a_1\rho\cos\theta)^2+\eta^2]^{1/2}}\mathrm{d}\theta\,\mathrm{d}\rho$$
$$-\frac{M\eta}{\pi}\,\mathrm{sh}\left(\frac{M\eta}{2}\right)\int_0^\xi\frac{K_1[(M/2)(t^2+\eta^2)^{1/2}]}{(t^2+\eta^2)^{1/2}}\mathrm{d}t, \tag{47}$$

$$B(\xi,\eta)=-\frac{2M\eta}{\pi^2}\,\mathrm{ch}\left(\frac{M\eta}{2}\right)a_1^2\int_0^1\rho\theta(\rho)\int_0^\pi\cos\theta\frac{K_1\{(M/2)[(\xi+a_1\rho\cos\theta)^2+\eta^2]^{1/2}\}}{[(\xi+a_1\rho\cos\theta)^2+\eta^2]^{1/2}}\mathrm{d}\theta\,\mathrm{d}\rho$$
$$+\frac{M\eta}{2}\,\mathrm{ch}\left(\frac{M\eta}{2}\right)\int_0^\xi\frac{K_1[(M/2)(t^2+\eta^2)^{1/2}]}{(t^2+\eta^2)^{1/2}}\mathrm{d}t. \tag{48}$$

We note that the singularities of the quantity $K_1\{(M/2)[(\xi+a_1\rho\cos\theta)^2+\eta^2]^{1/2}\}$ lie on the conducting part and that this singularity is of the 'double-layer' type.

RESULTS AND DISCUSSION

To find the value of B on the conducting part ($\eta=0$, $-a_1<\xi<a_1$), we substitute $A(\alpha)$ from equation (21) in equation (18) to give

$$B(\xi,0)=\frac{4}{\pi}\int_0^\infty\left(H(\alpha)+\frac{J_0(\alpha a_1)}{2\alpha}\right)\sin(\xi\alpha)\mathrm{d}\alpha \tag{49}$$

and, by using the representation of $H(\alpha)$ (equation (24)) with $\rho f(\rho a_1)=\rho\theta(\rho)+1/2a_1$, we get

$$B(\xi,0)=\frac{4a_1^2}{\pi}\int_0^\infty\int_0^1 \rho\theta(\rho)J_1(\alpha\rho a_1)\sin(\xi\alpha)\mathrm{d}\rho\,\mathrm{d}\alpha+\frac{4}{\pi}\int_0^\infty\frac{\sin(\xi\alpha)}{2\alpha}\mathrm{d}\alpha. \tag{50}$$

Changing the order of integrations and using the identity (27) and the identity

$$\int_0^\infty\frac{\sin(\xi\alpha)}{\alpha}\mathrm{d}\alpha=\begin{cases}\pi/2 & \text{if } \xi>0,\\ -\pi/2 & \text{if } \xi<0,\end{cases} \tag{51}$$

one can obtain

$$B(\xi,0)=\frac{4\xi a_1}{\pi}\int_{\xi/a_1}^1\frac{\theta(\rho)}{(\rho^2a_1^2-\xi^2)^{1/2}}\mathrm{d}\rho\pm 1;\quad \begin{cases}\xi>0\\ \xi<0.\end{cases} \tag{52}$$

By writing $\rho a_1=\xi\mathrm{ch}t$, $B(\xi,0)$ can be put in the form

$$B(\xi,0)=\frac{4}{\pi}\int_0^{\mathrm{arcch}(a_1/\xi)}\xi\theta\left(\frac{\xi}{a_1}\mathrm{ch}t\right)\mathrm{d}t\pm 1;\quad \begin{cases}\xi>0,\\ \xi<0,\end{cases} \tag{53}$$

and then numerical integration (Gauss–Legendre) was used. The function $\theta[(\xi/a_1)\mathrm{ch}t]$ was first interpolated using the points ρa_1 $(0<\rho<1,\ \rho=(x_{i+1})/2;\ x_i$ are the Gauss–Legendre abscissae) at the points $\xi\mathrm{ch}t/a_1$.

When $a_1=0$ (no conducting portion on the boundary), $V(\xi,\eta)$ and $B(\xi,\eta)$ become, from equations (47) and (48),

$$V(\xi,\eta)=-\frac{M\eta}{\pi}\mathrm{sh}\left(\frac{M\eta}{2}\right)\int_0^\xi\frac{K_1[(M/2)(t^2+\eta^2)^{1/2}]}{(t^2+\eta^2)^{1/2}}\mathrm{d}t, \tag{54}$$

$$B(\xi,\eta)=\frac{M\eta}{\pi}\mathrm{ch}\left(\frac{M\eta}{2}\right)\int_0^\xi\frac{K_1[(M/2)(t^2+\eta^2)^{1/2}]}{(t^2+\eta^2)^{1/2}}\mathrm{d}t. \tag{55}$$

Since

$$K_1\left(\frac{M}{2}(t^2+\eta^2)^{1/2}\right)\approx\frac{2}{M}\frac{1}{(t^2+\eta^2)^{1/2}}$$

for small t and η at the singularity point $(\xi,\eta)=(0,0)$ (the point where the value of B changes from -1 to 1), $V(\xi,\eta)$ and $B(\xi,\eta)$ behave as

$$V(\xi,\eta)\approx-\frac{2}{\pi}\eta\mathrm{sh}\left(\frac{M\eta}{2}\right)\int_0^\xi\frac{1}{t^2+\eta^2}\mathrm{d}t, \tag{56}$$

$$B(\xi,\eta)\approx\frac{2}{\pi}\eta\mathrm{ch}\left(\frac{M\eta}{2}\right)\int_0^\xi\frac{1}{t^2+\eta^2}\mathrm{d}t, \tag{57}$$

which are

$$V(\xi,\eta)=-\frac{2}{\pi}\mathrm{sh}\left(\frac{M\eta}{2}\right)\arctan\frac{\xi}{\eta}, \tag{58}$$

$$B(\xi,\eta)=\frac{2}{\pi}\mathrm{ch}\left(\frac{M\eta}{2}\right)\arctan\frac{\xi}{\eta}. \tag{59}$$

The Fredholm's integral equation (40) was discretized and solved with the kernel (41) and the right-hand-side function (42). The finite integrals in the Fredholm's equation (40) and in the kernel (41) were evaluated using the Gauss–Legendre quadrature formula. For Hartmann numbers $M=10$ and 20, 16 points were enough for the integration; for higher M, 24 points were used to obtain the desired accuracy.

Once $\rho\theta(\rho)=\rho f(\rho a_1)-1/2a_1$ values were obtained, they were substituted back in equations (47) and (48) and $V(\xi,\eta)$, $B(\xi,\eta)$ were computed at discrete points in the region $0\leqslant\xi\leqslant 1$ and $0\leqslant\eta\leqslant 1$ (since both V and B are antisymmetric with respect to the η-axis, computations are carried out in the quarter-plane $\xi\geqslant 0$, $\eta\geqslant 0$). The region $0\leqslant\xi\leqslant 1$, $0\leqslant\eta\leqslant 1$ was divided into 441 mesh points by taking the step sizes $\xi h=\eta h=0{\cdot}05$, and the velocity $V(\xi,\eta)$ and the magnetic field $B(\xi,\eta)$ were computed at these mesh points.

We present the equal-velocity lines for $a_1=0{\cdot}3$ and Hartmann numbers $M=10$, 50 and 100 in Figures 2, 3 and 4 respectively. One can notice from these figures that although this problem is solved for a half-plane, the flow is confined to a relatively small region near the line $\xi=a_1$. In the rest of the region the fluid is almost stagnant. Equal-magnetic-field lines (current lines) for the same Hartmann numbers are shown in Figures 5, 6 and 7 respectively. As M increases, a boundary layer is formed near the $\eta=0$ line for $\xi>a_1$ for both velocity and induced magnetic field. It can also be seen from these graphs that, except for narrow regions near $\eta=0$ and $\xi=0$, the velocity is almost constant and equal to its minimum value. Near the line $\xi=0$ these lines move towards it; however, for large values of η they will start bending away from the $\xi=0$ line, confirming that $|V|\to\infty$ as $\eta\to\infty$. The behaviour of the current lines is similar to that of the equal-velocity lines except for $\xi<a_1$ and for small values of η, because in this case the current lines are perpendicular to the ξ-axis owing to the boundary condition $\partial B/\partial\eta=0$. Also in most parts of the region the value of the magnetic field is stationary and equal to its maximum value. Since our mesh size is $\xi h=0{\cdot}05$, the lines which are between $\xi=0{\cdot}25$ and $\xi=0{\cdot}3=a_1$ are obtained from the

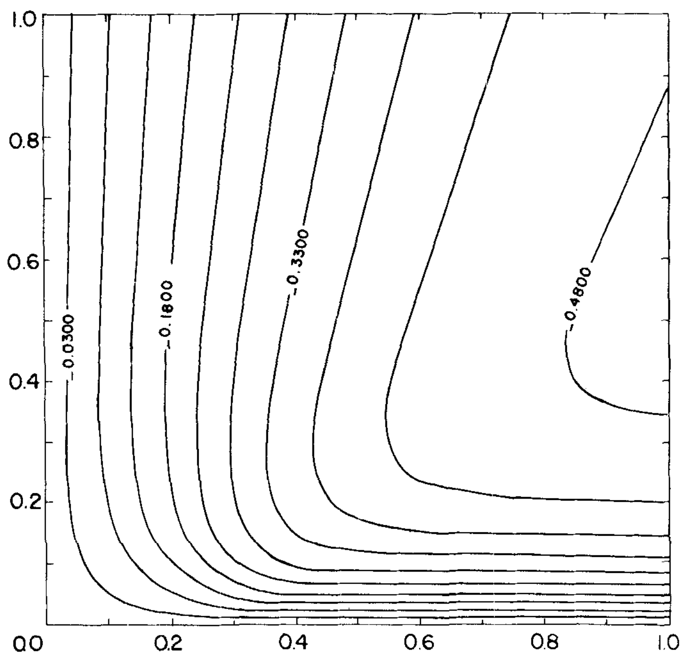

Figure 2. Velocity lines for $M=10$, $a_1=0{\cdot}3$

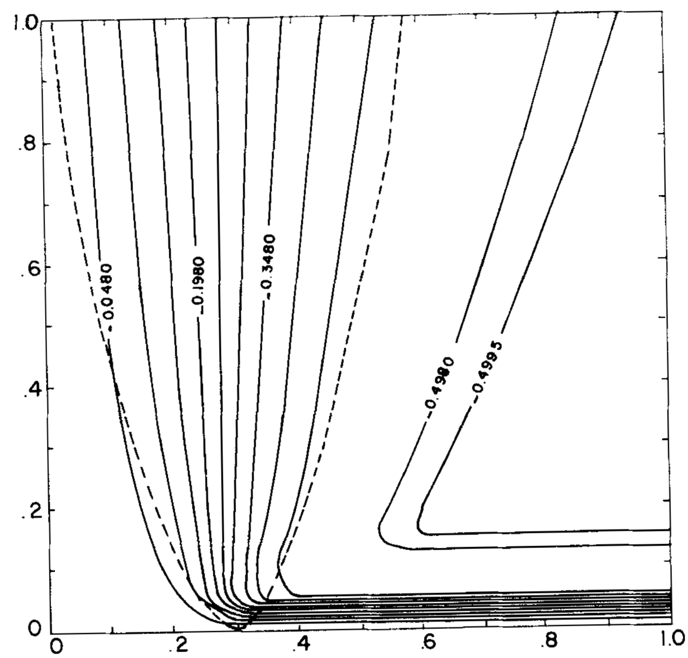

Figure 3. Velocity lines for $M=50$, $a_1=0{\cdot}3$; ---, the parabolic boundary layer

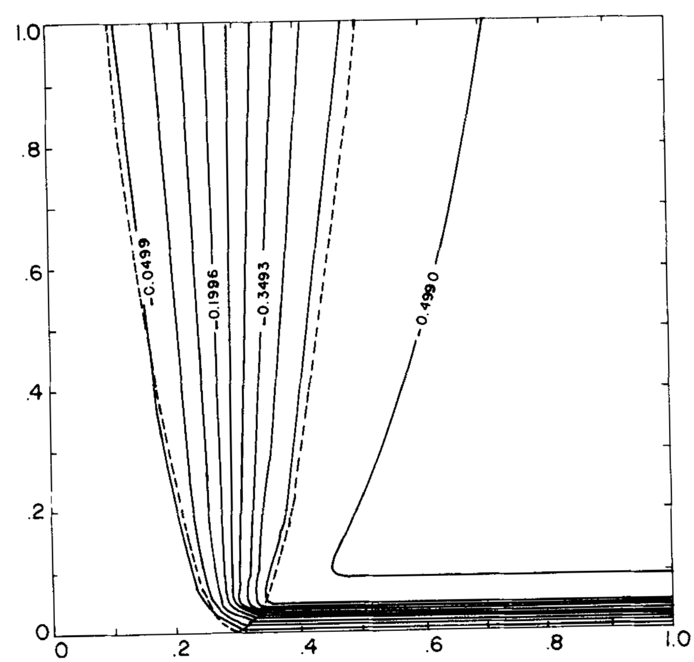

Figure 4. Velocity lines for $M=100$, $a_1=0{\cdot}3$; ---, the parabolic boundary layer

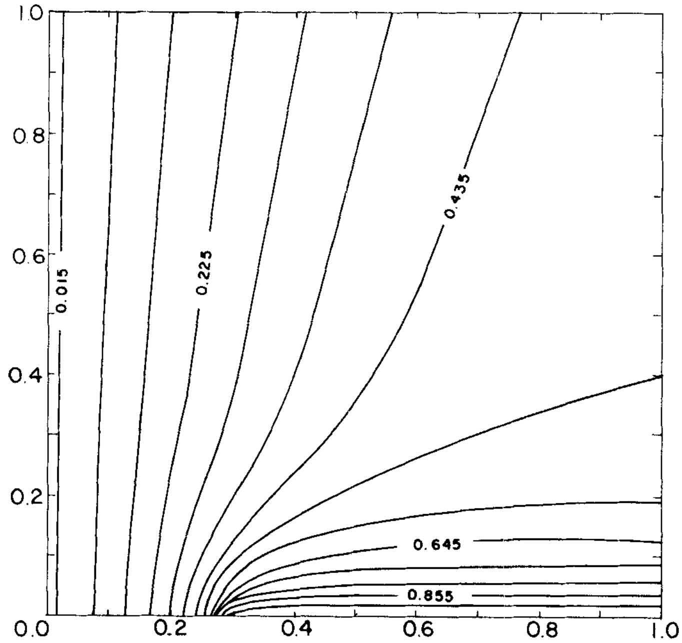

Figure 5. Magnetic field lines for $M=10$, $a_1=0.3$

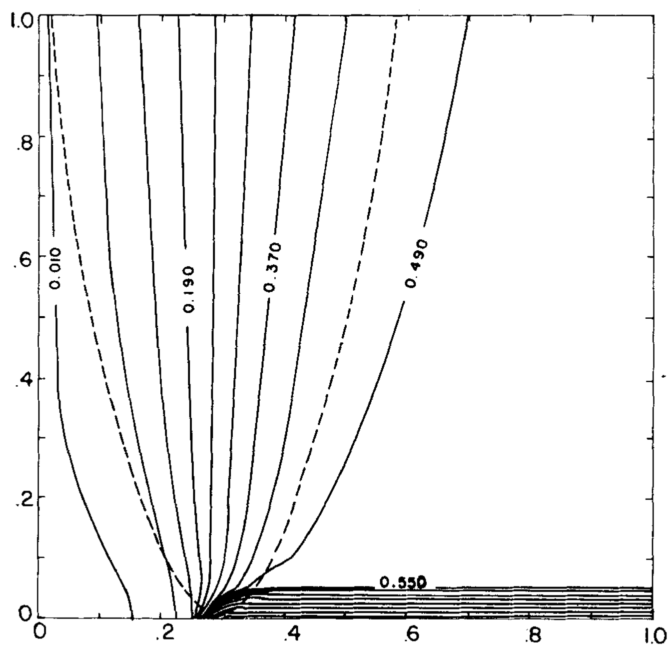

Figure 6. Magenetic field lines for $M=50$, $a_1=0{\cdot}3$; ---, the parabolic boundary layer

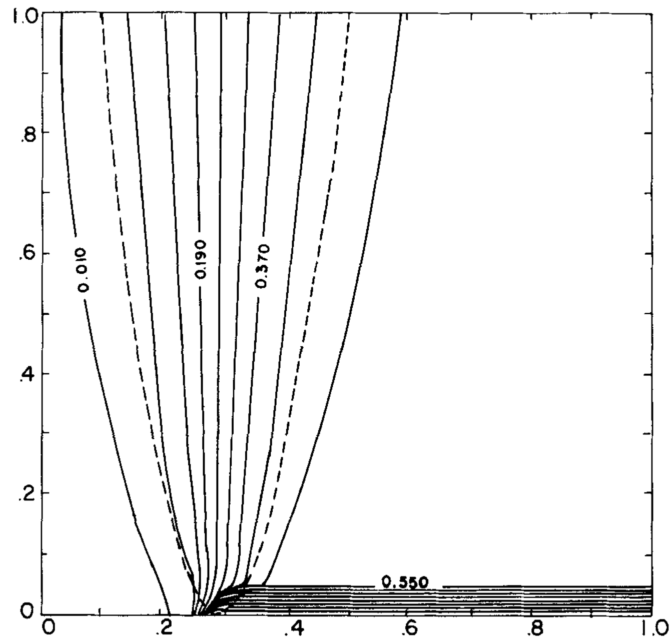

Figure 7. Magnetic field lines for $M=100$, $a_1=0{\cdot}3$; ---, the parabolic boundary layer

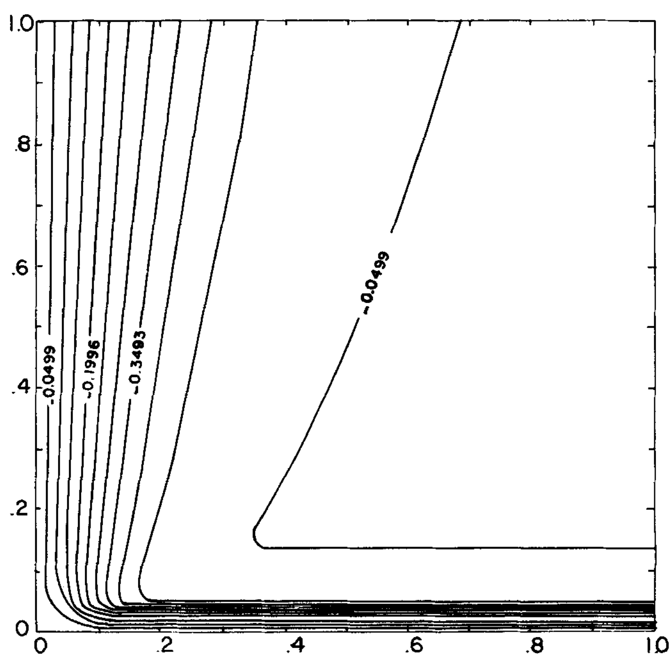

Figure 8. Velocity lines for $M=50$, $a_1=0{\cdot}1$

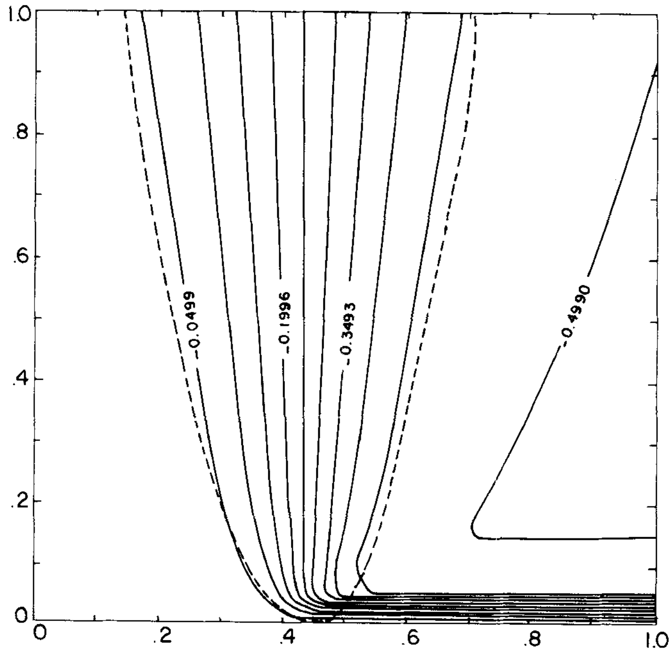

Figure 9. Velocity lines for $M = 50$, $a_1 = 0{\cdot}45$; ---, the parabolic boundary layer

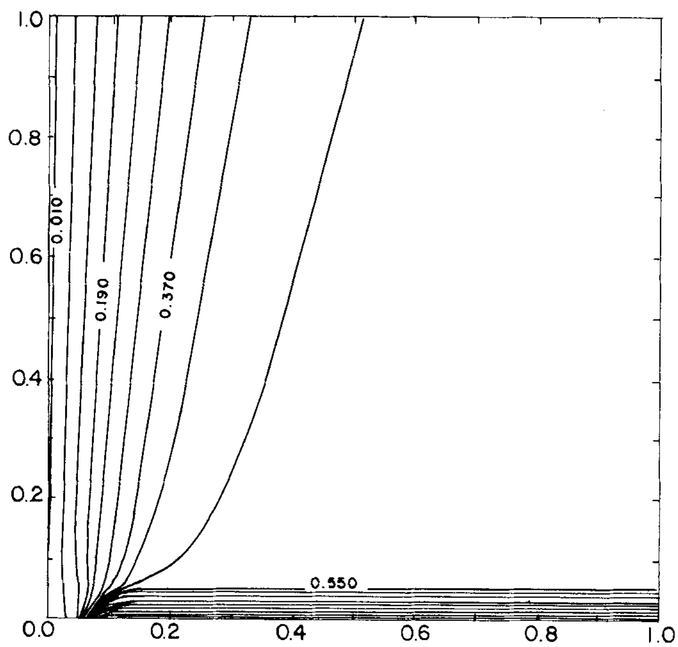

Figure 10. Magnetic field lines for $M = 50$, $a_1 = 0{\cdot}1$

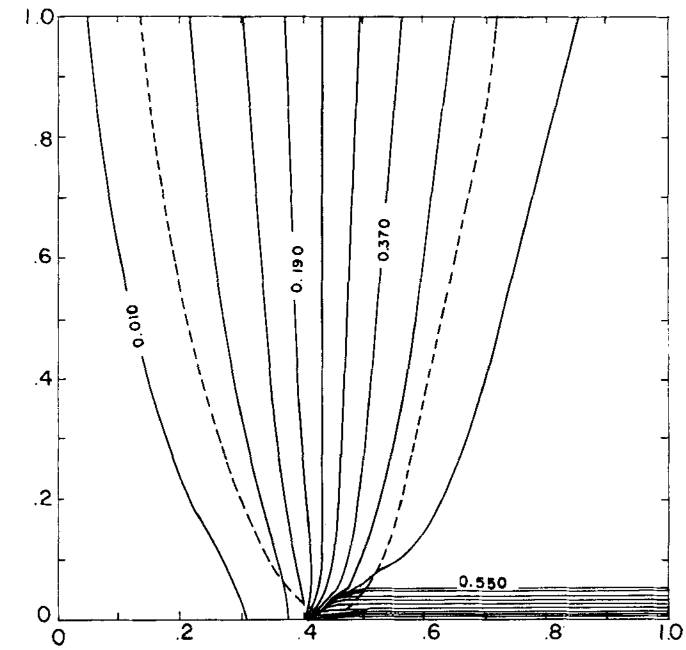

Figure 11. Magnetic field lines for $M=50$, $a_1=0{\cdot}45$; ---, the parabolic boundary layer

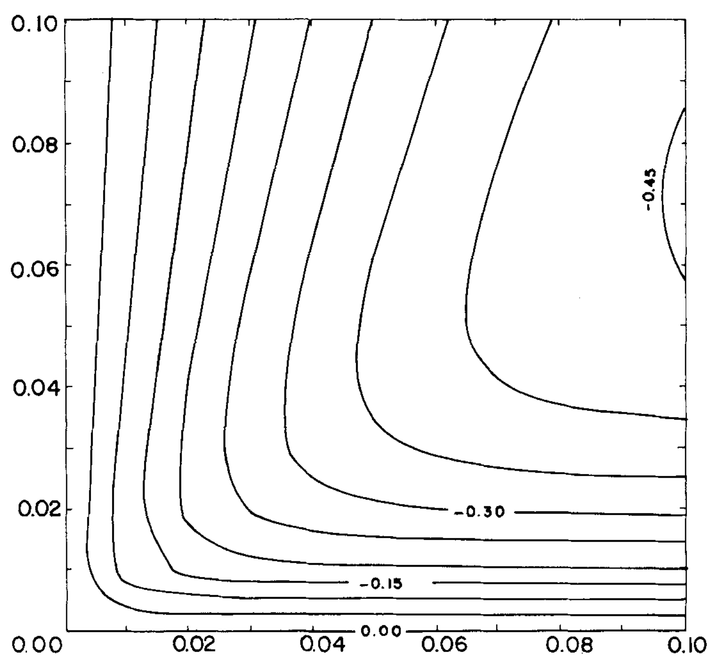

Figure 12. Velocity lines for $M=50$, $a_1=0{\cdot}0$; $0\leqslant\xi, \eta\leqslant 0{\cdot}1$

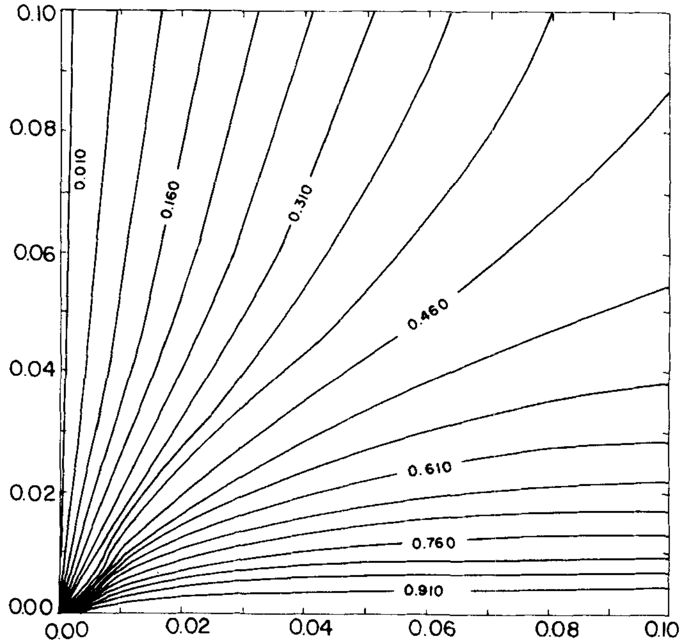

Figure 13. Magnetic field lines for $M=50$, $a_1=0{\cdot}0$; $0\leqslant\xi$, $\eta\leqslant 0{\cdot}1$

interpolation in the graphic program and this causes some error for these lines when they are close to the ξ-axis.

In Figures 8, 9 and 10, 11 equal-velocity lines and current lines are shown respectively for $M=50$ and for $a_1=0{\cdot}1$, $0{\cdot}45$, indicating the development of a stagnant region in front of the conducting wall when the conducting length a_1 is increased. For $a_1=0{\cdot}0$ equal-velocity lines and current lines are shown in Figures 12 and 13 respectively in a small square region $0\leqslant\xi\leqslant 0{\cdot}1$ and $0\leqslant\eta\leqslant 0{\cdot}1$. Current lines start from the origin, since $B(0,\eta)=0$ and $B(\xi,0)=1$, $\xi>0$, and confirm the behaviour indicated in equation (59).

Finally we notice the development of the parabolic boundary layer near $\xi=0$. For small values of a_1 and/or M this boundary layer interacts with the similar layer originating at $\xi=-a_1$. For higher values of a_1 and M, however, the two layers are separated, and the one in the first quadrant is indicated in Figures 3, 4, 6, 7, 9 and 11. It was difficult in this case to give details of the region in the neighbourhood of the point $(a_1, 0)$.

This problem is generalized in Sezgin[10] for MHD flow between parallel plates, where two electrodes of length $2a_1$ are placed in the middle of the plates symmetrically. When $a_1=0$, this problem reduces to the special case of the flow induced by line electrodes at $\xi=0$, $\eta=\pm 1$ set in insulating plates at $\eta=\pm 1$, with a magnetic field applied in the η-direction. This special case has been considered by Hunt and Williams[3] and our solution for $a_1=0$ coincides with theirs. In their paper they examine the asymptotic solution for large M in separate regions and their current lines in the core region compare well with our current lines for $a_1=0$.

ACKNOWLEDGEMENT

This work was supported by the Scientific and Technical Research Council of Turkey.

APPENDIX I

Consider

$$Q=\int_0^\infty (\beta^2+x^2)^{-1/2}e^{-\alpha(\beta^2+x^2)^{1/2}}\frac{J_1(\gamma x)}{x}\,dx; \tag{60}$$

then we have (Reference 9, p. 47)

$$\frac{d}{d\gamma}(\gamma Q)=\gamma\int_0^\infty (\beta^2+x^2)^{-1/2}e^{-\alpha(\beta^2+x^2)^{1/2}}J_0(\gamma x)\,dx=\gamma I_0(\beta p_-)K_0(\beta p_+). \tag{61}$$

Integrating with respect to γ, we get

$$Q\gamma=\tfrac{1}{2}\gamma^2[I_0(\beta p_-)K_0(\beta p_+)+I_1(\beta p_-)K_1(\beta p_+)]+\text{constant},$$

where the constant vanishes at $\gamma\to 0$. Hence

$$Q=\int_0^\infty (\beta^2+x^2)^{-1/2}e^{-\alpha(\beta^2+x^2)^{1/2}}\frac{J_1(\gamma x)}{x}\,dx=\tfrac{1}{2}\gamma[I_0(\beta p_-)K_0(\beta p_+)+I_1(\beta p_-)K_1(\beta p_+)]. \tag{62}$$

Taking the second derivative of Q with respect to α,

$$\int_0^\infty (\beta^2+x^2)^{1/2}e^{-\alpha(\beta^2+x^2)^{1/2}}\frac{J_1(\gamma x)}{x}\,dx=\tfrac{1}{2}\beta\gamma\{\beta[I_0(\beta p_-)K_0(\beta p_+)+I_1(\beta p_-)K_1(\beta p_+)]$$
$$+(\alpha^2+\gamma^2)^{-1/2}[I_0(\beta p_-)K_1(\beta p_+)-I_1(\beta p_-)K_0(\beta p_+)]\}. \tag{63}$$

Setting $\alpha=0$ ($p_-=p_+=\tfrac{1}{2}\gamma$), we get

$$\int_0^\infty (\beta^2+x^2)^{1/2}\frac{J_1(\gamma x)}{x}\,dx=\tfrac{1}{2}\beta\{\beta\gamma[I_0(\tfrac{1}{2}\beta\gamma)K_0(\tfrac{1}{2}\beta\gamma)+I_1(\tfrac{1}{2}\beta\gamma)K_1(\tfrac{1}{2}\beta\gamma)]$$
$$+[I_0(\tfrac{1}{2}\beta\gamma)K_1(\tfrac{1}{2}\beta\gamma)-I_1(\tfrac{1}{2}\beta\gamma)K_0(\tfrac{1}{2}\beta\gamma)]\}. \tag{64}$$

APPENDIX II

Consider the integral

$$R=\int_0^\infty e^{-k(u^2+\alpha^2)^{1/2}}\sin(\xi\alpha)\,J_1(\alpha x)\,d\alpha. \tag{65}$$

Since

$$J_1(z)=\frac{1}{\pi}\int_0^\pi \cos\theta\sin(z\cos\theta)\,d\theta,$$

the integral (65) can be written as

$$R=\frac{1}{\pi}\int_0^\infty e^{-k(u^2+\alpha^2)^{1/2}}\int_0^\pi \cos\theta\sin(\xi\alpha)\sin(\alpha x\cos\theta)\,d\theta\,d\alpha$$
$$=\frac{1}{2\pi}\int_0^\infty e^{-k(u^2+\alpha^2)^{1/2}}\int_0^\pi \cos\theta[\cos\alpha(\xi-x\cos\theta)-\cos\alpha(\xi+x\cos\theta)]\,d\theta\,d\alpha$$
$$=\frac{1}{2\pi}\int_0^\pi \cos d\theta\int_0^\infty e^{-k(u^2+\alpha^2)^{1/2}}[\cos\alpha(\xi-x\cos\theta)-\cos\alpha(\xi+x\cos\theta)]\,d\alpha. \tag{66}$$

For the evaluation of the infinite integrals above we make use of the identity[6]

$$\int_0^\infty e^{-\beta(\gamma^2+x^2)^{1/2}}\cos(ax)\frac{dx}{(\gamma^2+x^2)^{1/2}}=K_0[\gamma(a^2+\beta^2)^{1/2}]. \tag{67}$$

By taking the derivative of (67) with respect to β we arrive at

$$\int_0^\infty e^{-\beta(\gamma^2+x^2)^{1/2}}\cos(ax)\,dx=K_1[\gamma(a^2+\beta^2)^{1/2}]\frac{\gamma\beta}{(a^2+\beta^2)^{1/2}}. \tag{68}$$

Now substituting (68) back into (66), we get

$$R=\frac{uk}{2\pi}\int_0^\pi \cos\theta\left[\frac{K_1\{u[(\xi-x\cos\theta)^2+k^2]^{1/2}\}}{[(\xi-x\cos\theta)^2+k^2]^{1/2}}-\frac{K_1\{u[(\xi+x\cos\theta)^2+k^2]^{1/2}\}}{[(\xi+x\cos\theta)^2+k^2]^{1/2}}\right]d\theta$$

$$=-\frac{uk}{\pi}\int_0^\pi \cos\theta\frac{K_1\{u[(\xi+x\cos\theta)^2+k^2]^{1/2}\}}{[(\xi+x\cos\theta)^2+k^2]^{1/2}}\,d\theta.$$

Therefore

$$\int_0^\infty e^{-k(u^2+\alpha^2)^{1/2}}\sin(\xi\alpha)J_1(\alpha x)\,d\alpha=-\frac{uk}{\pi}\int_0^\pi \cos\theta\frac{K_1\{u[(\xi+x\cos\theta)^2+k^2]^{1/2}\}}{[(\xi+x\cos\theta)^2+k^2]^{1/2}}\,d\theta. \tag{69}$$

REFERENCES

1. L. Dragoş, *Magnetofluid Diynamics*, Abacus Press, 1975.
2. J. A. Shercliff, 'Steady motion of conducting fluids in pipes under transverse magnetic fields', *Proc. Camb. Phil. Soc.*, **49**, 136–144 (1953).
3. J. C. R. Hunt and W. E. Williams, 'Some electrically driven flows in MHD', *J. Fluid Mech.*, **31**, 705–722 (1968).
4. M. Abramowitz and I. A. Stegun, *Handbook of Mathematical Functions*, Dover Publications, New York, 1965.
5. I. N. Sneddon, *Mixed Boundary Value Problems in Potential Theory*, North-Holland, Wiley, New York, 1966.
6. I. S. Gradshteyn and I. M. Ryzhik, *Tables of Integrals, Series and Products*, Academic Press, New York and London, 1965.
7. G. Eason, B. Noble and I. N. Sneddon, 'On certain integrals of Lipschitz–Hankel type involving products of Bessel functions', *Phil. Trans. Roy. Soc., Series A*, **247**, 529–551 (1955).
8. M. Sezgin, 'Magnetohydrodynamic flow in an infinite channel', *Int. j. numer. methods fluids*, **6**, 593–609 (1986).
9. F. Oberhettinger, *Tables of Bessel Transforms*, Springer-Verlag, 1972.
10. M. Sezgin, 'Some mixed boundary value problems in MHD', *Ph.D. Thesis*, Calgary, 1983.